JACS
JOURNAL OF THE AMERICAN CHEMICAL SOCIETY

Communication

pubs.acs.org/JACS

Growth of Protein Crystals in Hydrogels Prevents Osmotic Shock

Shigeru Sugiyama,*[,†,‡,#] Mihoko Maruyama,[†,‡] Gen Sazaki,[†,‡,⊥] Mika Hirose,[†,‡] Hiroaki Adachi,[†,‡,§] Kazufumi Takano,[†,‡,§] Satoshi Murakami,[‡,§,∥] Tsuyoshi Inoue,[†,‡,§] Yusuke Mori,[†,‡,§] and Hiroyoshi Matsumura*[,†,‡,§]

[†]Graduate School of Engineering, Osaka University, Suita, Osaka 565-0871, Japan

[‡]Japan Science and Technology Agency, Suita, Osaka 565-0871, Japan

[§]SOSHO Inc., Suita, Osaka 565-0871, Japan

[∥] Graduate School of Bioscience and Biotechnology, Tokyo Institute of Technology, Nagatsuta, Midori-ku, Yokohama 226-8501, Japan

Supporting Information

ABSTRACT: High-throughput protein X-ray crystallography offers a significant opportunity to facilitate drug discovery. The most reliable approach is to determine the three-dimensional structure of the protein−ligand complex by soaking the ligand in apo crystals. However, protein apo crystals produced by conventional crystallization in a solution are fatally damaged by osmotic shock during soaking. To overcome this difficulty, we present a novel technique for growing protein crystals in a high-concentration hydrogel that is completely gellified and exhibits high strength. This technique allowed us essentially to increase the mechanical stability of the crystals, preventing serious damage to the crystals caused by osmotic shock. Thus, this method may accelerate structure-based drug discoveries.

Once the three-dimensional (3D) structure of a target protein has been determined, it is then important to identify the active site and the binding sites of key ligand molecules. The most reliable approach for such identification is to determine the 3D structure of protein complexes produced by soaking ligand molecules in apo crystals.[1−3] However, macromolecular crystallography for drug discovery faces a serious problem: protein crystals tend to suffer significant damage during soaking.[4−8] Since most lead compounds are not readily water-soluble, they must be dissolved in high-concentration organic solvents such as alcohol and dimethyl sulfoxide (DMSO). Therefore, to date, it has been impossible to produce crystals of complexes of the target protein and such lead compounds by soaking in high-concentration organic solvents containing the lead compounds because the protein crystals dissolve in such solvents immediately.[9,10] This problem arises from the sensitivity of protein crystals to osmotic shock, which causes serious changes in the crystal packing. We recently developed a new method for growing protein crystals in a high-concentration hydrogel, in relation to an automated system for processing protein crystals using a femtosecond laser.[11−18] We could handle protein crystals without touching them directly during the experiments, resulting in a significant reduction in physical damage to the crystals. Furthermore, the hydrogel-grown crystals could be easily captured from the solution using a cryoloop and immediately mounted onto the goniometer head of the X-ray diffraction (XRD) equipment because the hydrogel surrounding the crystals protected them while serving as an anchor to fix a crystal on a cryoloop. Those crystals could also be stored for later reuse after the diffraction experiments. Here we present the important characteristics of hydrogel-grown crystals, demonstrating that these crystals can overcome a significant problem caused by soaking. Interestingly enough, we found that this method enabled us essentially to increase the mechanical stability of the crystals while considerably reducing the osmotic shock.

Protein crystals dissolve immediately when they are soaked in high-concentration organic solvents and high-ionic-strength solutions, which are substantially different from those inducing crystal growth.[5] Nevertheless, glucose isomerase (GI) and lysozyme (LZM) crystals grown in hydrogel did not dissolve for more than 30 min when transferred to buffer-free solutions containing 60% (v/v) DMSO, 100% methanol, 100% glycerol, or nearly saturated 5 M lithium acetate [Figure 1A−D and Figure S1 in the Supporting Information (SI)]. We also observed that hydrogel-grown elastase (ELS) and thaumatin (ThM) crystals did not dissolve under the same conditions. They exhibited sharp edges and vertices, as observed under a stereoscopic microscope. In contrast, solution-grown crystals dissolved immediately in these solutions.

Furthermore, a two-beam interferometer[19] was used to measure the diffusion rates of these buffer-free solutions in hydrogel. The results revealed that both the high-concentration organic solvents and high-ionic-strength solutions penetrate into crystals in the hydrogel. The evaluated diffusion coefficients are summarized in Table S1 in the SI. To clarify whether the hydrogel surrounding the crystals reduces the influence of osmotic shock by protecting the crystals from the buffer-free solutions, we processed the LZM and ThM crystals themselves grown in hydrogel using the femtosecond laser processing system (Figure S2). The processed hydrogel-grown LZM and ThM crystals were then soaked in buffer-free solutions containing 60% (v/v) DMSO and 5 M lithium

Received: February 17, 2012
Published: March 21, 2012

dx.doi.org/10.1021/ja301584y | J. Am. Chem. Soc. 2012, 134, 5786−5789

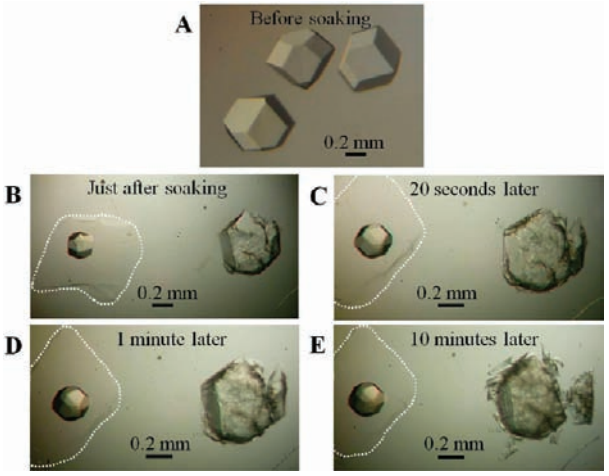

Figure 1. Soaking experiments with hydrogel-grown GI crystals. (A) Solution-grown crystals before they were transferred to the solution. (B–E) Two crystals were transferred to a buffer-free solution of 5 M lithium acetate at almost the same time. The left (right) crystal is a hydrogel-grown (solution-grown) crystal. The white dotted lines indicate the border between the hydrogel and the solution. The crystals were soaked in the solution at 293 K. (B) The solution-grown crystal began to dissolve soon after being transferred to the solution, whereas no cracks or dissolution were observed on the surface of the hydrogel-grown crystal. (C, D) The dissolution of the solution-grown crystal continued, whereas the hydrogel-grown crystal retained sharp edges and vertices. (E) The solution-grown crystal was completely disrupted in 10 min, but the shape of the hydrogel-grown crystal remained intact.

acetate, respectively. It is noteworthy that the processed crystals remained undissolved for more than 30 min in these solutions even though the crystals were not partially surrounded by the hydrogel.

Next, XRD experiments were performed to examine the diffraction quality of the hydrogel-grown crystals soaked in buffer-free solutions. The hydrogel-grown crystals were successfully cooled in flash-cooling processes using a cryoloop (Figure 2A–D). The XRD pattern featured sharp, clear diffraction spots without streaks or breaks (Figure 2A–D). In general, when protein crystals are soaked in high-concentration organic solvents and high-ionic-strength solutions, large lattice stresses are introduced into the crystals, resulting in shrinkage of the unit cell.[5−7] However, the unit cell dimensions of the hydrogel-grown crystals were almost the same as those deposited in the Protein Data Bank (PDB) (Tables S2 and S3). These results indicate that the hydrogel-grown crystals can sufficiently withstand osmotic pressure. We also confirmed by XRD experiments that the laser-processed hydrogel-grown crystals can tolerate osmotic pressure. Surprisingly, the hydrogel-grown GI (space groups $I222$ and $P2_12_12$) and ELS crystals afforded diffraction data at the highest resolution hitherto reported for them even though these crystals were soaked in a buffer-free solution of 5 M lithium acetate (Table S2). The hydrogel-grown ThM crystal also exhibited the second highest resolution (0.96 Å).

In XRD measurements under cryogenic conditions, the processed hydrogel-grown LZM and ThM crystals were exposed to 50 μm focused X-ray beams in two positions located approximately 50 and 200 μm from the processing surface (Figure S2A,B). Consequently, a comparison of the XRD data statistics was almost the same in the two different

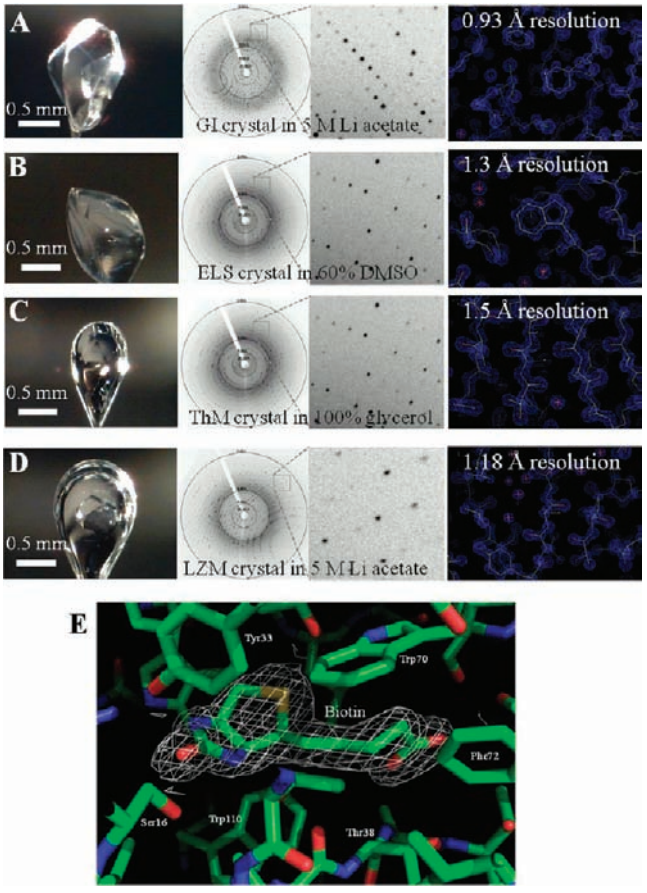

Figure 2. XRD experiments with hydrogel-grown crystals. (A–D) Photographs and XRD patterns of hydrogel-grown crystals at 100 K mounted by cryoloop. The electron-density maps contoured at 3.0σ were computed using the coefficients $2|F_o| - |F_c|$ and phases α_c after refinement. (A) GI crystal after soaking in 5 M lithium acetate. (B) ELS crystal after soaking in 60% (v/v) DMSO. (C) ThM crystal after soaking in 100% glycerol. (D) LZM crystal after soaking in 5 M lithium acetate. (E) Biotin binding model with the $2|F_o| - |F_c|$ omit map. The biotin electron density was calculated at 1.8 Å resolution.

positions (Table S4). These findings indicate that the XRD quality of a processed hydrogel-grown crystal is not affected by soaking it in high-concentration organic solvents and hign-ionic-strength solutions even if the crystal is not partially surrounded by the hydrogel. These data suggest that hydrogel-grown crystals have a greater capacity to tolerate environmental changes than do other solution-grown crystals.

Structural analyses were performed to examine the influence of osmotic shock on crystal packing during soaking. Clear, well-separated electron densities were observed (Figure 2 A–D). The 3D structures determined from the hydrogel-grown crystals were superimposed very well on those deposited in the PDB. The root-mean-square deviation (rmsd) between the monomers of GI $I222$-form crystals was evaluated to be 0.19 Å for 386 Cα atoms, and the rmsd between the two dimers of GI $P2_12_12$-form crystals was 0.28 Å for 772 Cα atoms. The rmsd between the ELS structures was 0.28 Å for 240 Cα atoms, and that between the ThM structures was 0.42 Å for 206 Cα atoms. These results demonstrate that the 3D structures determined from hydrogel-grown crystals are essentially the same as the high-resolution structures determined from solution-grown crystals.

dx.doi.org/10.1021/ja301584y | J. Am. Chem. Soc. 2012, 134, 5786−5789

We hypothesized that the mechanical properties of hydrogel-grown crystals may essentially differ from those of solution-grown crystals. To verify this, micro-Vickers hardness indentation measurements[20] were performed on hydrogel-grown and solution-grown LZM crystals. Indentations were made on the (110) face of the hydrogel-grown crystal (Figure 3B). The average value of the micro-Vickers hardness was estimated to be 21.6 MPa for the hydrogel-grown crystals. In contrast, no indentations could be made on the solution-grown crystals because the crystals were immediately disrupted even under the minimum load of the apparatus (Figure 3A). These results demonstrate that the hardness of hydrogel-grown crystals is significantly greater than that of solution-grown crystals.

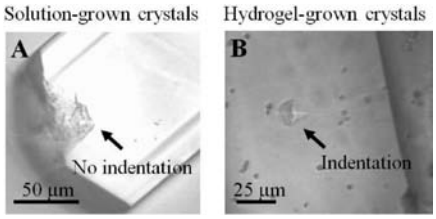

Figure 3. Comparison of the hardness of hydrogel-grown and solution-grown crystals. Micro-Vickers hardness indentation measurements were performed on solution-grown and hydrogel-grown LZM crystals in the wet condition at 293 K. These experiments were repeated for three trials for each loading on the hydrogel-grown and solution-grown crystals. (A) (110) face of a solution-grown LZM crystal. No indentations were made because the crystal was immediately disrupted even under the minimum load of the apparatus. (B) (110) face of an LZM crystal grown in hydrogel. The average value of the microhardness was 21.6 MPa.

Furthermore, hydrogel-grown and solution-grown LZM crystals were slightly dissolved by increasing the temperature, and their surface morphologies were observed by laser confocal microscopy.[21] The solution-grown crystals exhibited deep etch pits at 303 K (Figure 4A), while the hydrogel-grown crystals exhibited etch pits at a higher temperature (305 K: Figure 4B,D). In addition, the density of the etch pits on the solution-grown crystals at 305 K (Figure 4C) was significantly higher than that on the hydrogel-grown crystals at the same temperature (Figure 4D). These results demonstrate that the hydrogel-grown crystals are more tolerant of temperature changes than those grown in solution, agreeing quite well with the experimental result that the hydrogel-grown crystals could survive high-concentration organic solvents and high-ionic-strength solutions.

To learn whether protein crystals trap the hydrogel into themselves, we examined the entire dissolution process of a hydrogel-grown LZM crystal under a stereoscopic microscope. A crystal-free hydrogel after dissolution was observed in the same shape and size as the original crystal (Figure 5). These results clearly demonstrate that gel fibers were incorporated into the crystal during growth, resulting in significant strengthening of the mechanical properties of the crystal. Indeed, Garcia-Ruiz et al.[22] previously reported that the mechanical properties and stability of LZM crystals against dehydration are improved by the incorporation of a hydrophilic silica polymeric network. Interestingly, the etch pits appearing on the hydrogel-grown crystals exhibited a hexagonal shape that has never been observed on the solution-grown crystals (where lens-shaped etch pits usually appear[23]).

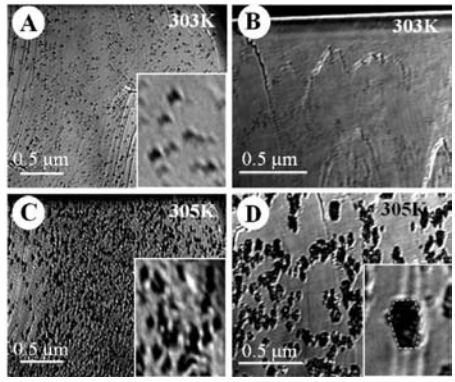

Figure 4. Laser confocal microscopy images of the (110) faces of LZM crystals showing changes in the surface morphology in situ for LZM crystals grown in (A, C) solution and (B, D) 0.25% (w/v) hydrogel. (A) Deep etch pits started to appear at 303 K on the surface of the solution-grown crystals, and subsequently the crystals dissolved. (B) The hydrogel-grown crystals did not exhibit deep etch pits or the retreat of growth steps on the crystal surfaces at 303 K. The crystals were unchanged during the observation. (C) The solution-grown crystals dissolved significantly at 305 K, and later the entire surface of the crystal was covered with deep pits at extremely high density. (D) The etch pits were observed on the hydrogel-grown crystal surfaces at 305 K.

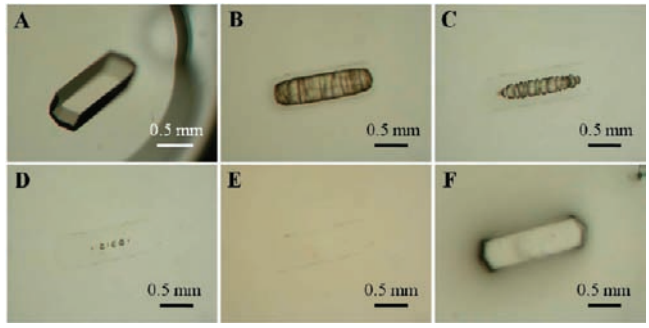

Figure 5. Dissolution of a hydrogel-grown LZM crystal. (A) Hydrogel-grown crystal before the dissolution experiment. Single crystals were excised from the hydrogel, and the surrounding extra hydrogel was removed. (B–D) The crystals were then transferred into deionized water to dissolve. (E) The LZM crystal was completely dissolved. (F) The remaining crystal-free hydrogel after the surrounding water was removed. The crystal-free hydrogel exhibited the same shape and size as the original LZM crystal. These observations demonstrate that the gel matrix and crystalline component coexist inside the hydrogel-grown crystals without disruption of the hydrogel network.

To investigate the general utility of this technique, hydrogel-grown apo-avidin crystals were transferred into a 10% DMSO solution containing a biotin ligand. We observed sharp edges and vertices of the hydrogel-grown crystals in a 10% DMSO solution, whereas the solution-grown apo-avidin crystals were immediately dissolved when soaked in the same solution. The 3D structure of the soaked crystal was analyzed at 1.8 Å resolution (Table S5), revealing a clear electron density map of the biotin bound to the active site (Figure 2E). This result suggests that the present technology is capable of solving the structures of complexes between target proteins and lead compounds when the apo crystals are soaked in a high-concentration organic solvent.

This new technology would be most effectively applied when introducing less-water-soluble lead compounds by soaking. It

dx.doi.org/10.1021/ja301584y | J. Am. Chem. Soc. 2012, 134, 5786–5789

could be also used as a powerful tool for successfully cooling large or mechanically unstable protein crystals for cryoprotection, particularly in very high resolution X-ray and neutron crystallography.

■ ASSOCIATED CONTENT

Supporting Information

Experimental details, including crystallization, femtosecond laser processing, XRD, structure determinations and refinements, micro-Vickers hardness of LZM crystals, and in situ observations by laser confocal microscopy. This material is available free of charge via the Internet at http://pubs.acs.org.

■ AUTHOR INFORMATION

Corresponding Author

sugiyama@chem.eng.osaka-u.ac.jp; matsumura@chem.eng.osaka-u.ac.jp

Present Addresses

[#]JST, ERATO, Murata Lipid Active Structure Project, Graduate School of Science, Osaka University, Japan.

[⊥]Laboratory for Phase Transition Dynamics of Ice, The Institute of Low Temperature Science, Hokkaido University, Japan.

Notes

The authors declare no competing financial interest.

■ ACKNOWLEDGMENTS

We thank Y. Umena, E. Yamashita, and A. Nakagawa on BL44XU and K. Baba and N. Mizuno on BL38B1 for the data collection at SPring-8 (Hyogo, Japan) and the staff members on NW12A for data collection at PF-AR (Tsukuba, Japan). The synchrotron radiation experiments were performed at SPring-8 with the approval of the Japan Synchrotron Radiation Research Institute (JASRI) (Proposal 2010B1261). This work was partially supported by a Core Research for Evolutional Science and Technology (CREST) Grant to Y.M., the Science and Technology Incubation Program of the Japan Science and Technology Agency to H.M., and Grants-in-Aid for Research Activity Start-up (Grant 23860028 to S.S.) from the Japan Society for the Promotion of Science.

■ REFERENCES

(1) Carr, R.; Jhoti, H. *Drug Discovery Today* **2002**, *7*, 522.

(2) Stewart, L.; Clark, R.; Behnke, C. *Drug Discovery Today* **2002**, *7*, 187.

(3) Goodwill, K. E.; Tennant, M. G.; Stevens, R. C. *Drug Discovery Today* **2001**, *6*, S113.

(4) Mitchell, E. P.; Garman, E. F. *J. Appl. Crystallogr.* **1994**, *27*, 1070.

(5) Lopez-Jaramillo, F. J.; Moraleda, A. B.; Gonzalez-Ramirez, L. A.; Carazo, A.; Garcia-Ruiz, J. M. *Acta Crystallogr.* **2002**, *D58*, 209.

(6) Frauenfelder, H.; Hartmann, H.; Karplus, M.; Kuntz, I. D.; Kuriyan, J.; Parak, F.; Petsko, G. A.; Ringe, D.; Tilton, R. F.; Connolly, M.; Max, N. *Biochemistry* **1987**, *26*, 254.

(7) Kurinov, I. V.; Harrison, R. W. *Acta Crystallogr.* **1995**, *D51*, 98.

(8) Kriminski, S.; Caylor, C. L.; Nonato, M. C.; Finkelstein, K. D.; Thorne, R. E. *Acta Crystallogr.* **2002**, *D58*, 459.

(9) Yao, M.; Yasutake, Y.; Tanaka, I. *Acta Crystallogr.* **2004**, *D60*, 39.

(10) Berejnov, V.; Husseini, N.; Alsaied, O. A.; Thorne, R. E. *J. Appl. Crystallogr.* **2006**, *39*, 244.

(11) Sugiyama, S.; Tanabe, K.; Hirose, M.; Kitatani, T.; Hasenaka, H.; Takahashi, Y.; Adachi, H.; Takano, K.; Murakami, S.; Mori, Y.; Inoue, T.; Matsumura, H. *Jpn. J. Appl. Phys.* **2009**, *48*, No. 075502.

(12) Sugiyama, S.; Hasenaka, H.; Hirose, M.; Shimizu, N.; Kitatani, T.; Takahashi, Y.; Adachi, H.; Takano, K.; Murakami, S.; Inoue, T.; Mori, Y.; Matsumura, H. *Jpn. J. Appl. Phys.* **2009**, *48*, No. 105502.

(13) Hasenaka, H.; Sugiyama, S.; Hirose, M.; Shimizu, N.; Kitatani, T.; Takahashi, Y.; Adachi, H.; Takano, K.; Murakami, S.; Mori, Y.; Inoue, T.; Matsumura, H. *J. Cryst. Growth* **2010**, *312*, 73.

(14) Yoshikawa, H. Y.; Murai, R.; Sugiyama, S.; Sazaki, G.; Kitatani, T.; Takahashi, Y.; Adachi, H.; Matsumura, H.; Murakami, S.; Inoue, T.; Takano, K.; Mori, Y. *J. Cryst. Growth* **2009**, *311*, 956.

(15) Tanabe, K.; Hirose, M.; Murai, R.; Sugiyama, S.; Shimizu, N.; Maruyama, M.; Takahashi, Y.; Adachi, H.; Takano, K.; Murakami, S.; Mori, Y.; Mizohata, E.; Inoue, T.; Matsumura, H. *Appl. Phys. Express* **2009**, *2*, No. 125501.

(16) Murai, R.; Yoshikawa, H. Y.; Takahashi, Y.; Maruyama, M.; Sugiyama, S.; Sazaki, G.; Adachi, H.; Matsumura, H.; Murakami, S.; Inoue, T.; Takano, K.; Mori, Y. *Appl. Phys. Lett.* **2010**, *96*, No. 043702.

(17) Matsumura, H.; Sugiyama, S.; Hirose, M.; Kakinouchi, K.; Maruyama, M.; Adachi, H.; Murai, R.; Takano, K.; Murakami, S.; Mori, Y.; Inoue, T. *Cryst. Growth Des.* **2011**, *11*, 1486.

(18) Sugiyama, S.; Hirose, M.; Shimizu, N.; Niiyama, M.; Maruyama, M.; Sazaki, G.; Murai, R.; Adachi, H.; Takano, K.; Murakami, S.; Inoue, T.; Mori, Y.; Matsumura, H. *Jpn. J. Appl. Phys.* **2011**, *50*, No. 025502.

(19) Sazaki, G.; Nagatoshi, Y.; Suzuki, Y.; Durbin, S. D.; Miyashita, S.; Nakada, T.; Komatsu, H. *J. Cryst. Growth* **1999**, *196*, 204.

(20) Koizumi, H.; Kawamoto, H.; Tachibana, M.; Kojima, K. *J. Phys. D: Appl. Phys.* **2008**, *41*, No. 074019.

(21) Sazaki, G.; Tsukamoto, K.; Yai, S.; Okada, M.; Nakajima, K. *J. Cryst. Growth* **2004**, *262*, 536.

(22) Garcia-Ruiz, J. M.; Gavira, J. A.; Otalora, F.; Guasch, A.; Coll, M. *Mater. Res. Bull.* **1998**, *33*, 1593.

(23) Honda, H.; Nakada, T. *Jpn. J. Appl. Phys.* **2004**, *43*, 4529.